

## High Temperature Ablation of Composite Material under Plasma Jet Impact

Rimantas LEVINSKAS\*, Romualdas KEZELIS, Kristina BRINKIENE,  
Viktorija GRIGAITIENE, Vitas VALINCIUS, Irena LUKOSIUTE,  
Zydrunas KAVALIAUSKAS, Arunas BALTUSNIKAS

Lithuanian Energy Institute, Breslaujos 3, LT-44403 Kaunas, Lithuania

**crossref** <http://dx.doi.org/10.5755/j01.ms.17.4.781>

Received 25 May 2011; accepted 19 June 2011

Simulation of the temperature distribution on space vehicles surfaces during its reentry phase is most important for assessing its landing safety. Recently composite materials, produced from high temperature resistance composites are under intensive investigations as surface protective shell for space vehicles during its reentry phases into the atmosphere. The main goal of research is to imitate high aerodynamic heating rates encountered by the protective material during reentry phases of space vehicles. This paper reports the experimental investigations of the new composite material based on light silicate frame impregnated by polymer composite tested in high temperature air jet, and generated by means of plasma torch. During experiments the plasma parameters were as follows: plasma torch capacity – (50–70) kW, air flow rate – (19–23) g/s, temperature – (1320–2420) °C, velocity – (40–50) m/s. To analyze the effect of the plasma jet impact to protective composite shell, the high speed camera movies were used. Temperature of samples set surface was measured using Type K (chromel/alumel) thermocouples. Data of composite material ablation rate and temperature of protective sample set surface during experiment are presented.

*Keywords:* plasma jet, protective shell, silicate composite, thermal resistance, ablation, XRD.

### 1. INTRODUCTION

High temperature ceramics are widely used in extreme environments. Ceramics being used for aerospace area must withstand high heat fluxes and a lot of wear, thus ceramic composites with good oxidation and thermal shock resistance, dimensional stability and ablation resistance are requested [1]. The great interest in space investigations has created a need for new advanced heat shield materials capable to efficiently protect Cube Sat landing probes from very high heating conditions under reentry into the Earth atmosphere [2]. Ultra-high temperature carbide/boride composites are considered as emerging materials for aerospace applications [3, 4]. Silicate based materials are perspective engineering materials suitable for many high temperature environment applications due to their high thermal shock resistance, chemical and physical durability, as well as stable and low thermal expansion coefficient [5]. Calcium silicates with light density, high strength, low thermal conductivity and endurance to high temperature are widely used as hard insulation for fire protection in many industries [6]. Light-weight insulation is an ideal material for use in the metallic thermal protection system not only on Reusable Launch Vehicles; it can also sustain severe aerodynamic heating during reentry into the atmosphere [7, 8]. Metallic thermal protection systems, consisting of a metallic shell panel fabricated from the high temperature alloy and light-weight insulation, are used to limit the maximum temperature of the vehicle during reentry [2, 9]. However, limited information about thermal properties of low weight insulation under environmental conditions are exposed. For the characterization of these materials thermal properties, including thermal stability

and thermal conductivity, XRF, spectral and microscopic analysis were used [6]. According to [10, 11] one of the key parameters for thermal characterization of light-weight ablators is a study of ablation resistance.

During the initial stages of reentry the probe's velocity is hypersonic while the atmosphere is essentially stagnant [12]. This causes intensive probe surface heating and pressurizing of the atmospheric gases surrounding the probe, which challenge a highly complex fluid, chemical, and heat transfer flows. Thermal protection materials (TPM) insulate Cube Sat probes surface from the overheating experienced during the reentry phase into Earth atmosphere [12, 13]. Nowadays it is very important to develop new light and effective TPM materials, especially for Cube Sat type satellites [2]. As predominant TPM of thermal and physical protection from the severe conditions that Cube Sat encounters upon atmospheric reentry could be high temperature resistance and very low thermal conductivity composite materials with high ablative properties at high temperatures. For this aim the compounds such as nylon – phenolics, teflon – teflons, carbon materials, carbon – phenolics, silica – teflon, inorganics and organics – silicone binders and other are applied [2]. Very perspective is the development of composite TPM based on high temperature resistance carbon or alumina based ceramics nano fibre bonded by various resins [2].

Recent advances in polymer layered silicate nanocomposites, especially with the improved thermal stability, flame retardancy and enhanced barrier properties promote the investigation of these materials as potential ablatives. Introduction of the layered nanosilicates (montmorillonite, tobermorite) into polymer matrix results in the increase of thermal stability of polymer nanocomposites and ablation resistance, which are not observed in each component [14].

\*Corresponding author. Tel.: +370-37-401804; fax.: +370-37-351271.  
E-mail address: [levin@mail.lei.lt](mailto:levin@mail.lei.lt) (R. Levinskas)

The other very important question is testing of TPM in real conditions. This testing is very complicated and expensive or, in some cases, in fact, impossible. Such facilities as discharge arc, shock tubes, ballistic ranges are used for the experimental testing of TPM [15–17]. Analytical models are used too, but in all cases experimental tests are performed. Arc-jet testing represents the best simulation of the reentry environment [3]. By this method not only the material response to large heat fluxes is evaluated, but the oxidation behavior under extreme conditions can be explored, too. The surface temperatures evaluated during the test are carried out to characterize the behavior of the material at typical atmospheric reentry conditions – high temperature, low pressure and oxidizing environment [3]. Problems under investigation include flow, temperature and heat flux measurements, TPM mechanical properties. These results are pointed out to evaluate the potential of the composite to withstand the reentry conditions with the temperatures higher than 2000 °C for a few minutes [3].

In addition, the ablation resistance is very important characteristic in the development of ceramic composites as insulation material for protecting the spacecraft elements against the aerodynamic heating during the reentry into the planetary atmosphere [18]. However, the ablation mechanism of silicate ceramics is still not well studied, especially for the high temperatures >2000 °C. In order to evaluate the thermal protection of the silicate composite at elevated temperatures, the ablation resistance of the materials was investigated. Plasma jet was used for the simulation of the high temperature ablation conditions for the atmospheric reentry flights. The changes in the surface temperature, ablation rate and mineral phase analysis were investigated in this study.

## 2. EXPERIMENTAL

The experiments of high temperature resistance composite material behavior under high velocity and temperature gas jet impact were carried out in the plasma jet generated by DC plasma torch. The plasma torch, generating the non-equilibrium plasma jet at atmospheric pressure, and its supplying equipment are described in detail in [19, 20]. The tested samples were mounted on the set made of alumina and placed in front of the expanding channel (Fig. 1).

The main operating parameters of the plasma torch are: power supply ( $P$ ) – (70–120) kW, arc current ( $I$ ) – (120–300) A, voltage ( $U$ ) – (250–400) V, total air flow rate ( $G$ ) – (10–30)  $\text{gs}^{-1}$ , the average outlet temperature ( $T$ ) – (1220–3220) °C, velocity ( $v$ ) – (30–1250) m/s. The distance between the channel outlet and the test samples was 0.01 m, channel diameter 0.06 m, samples geometry – (0.06 × 0.06 × 0.03) m. Two types of samples were tested: with protective shell N1, N2 (Fig. 1, a) and test bodies with protective reinforcement coating N1C, N2C (Fig. 1, b).

Protective shell was made of light silicates (mixture of 35 wt% tobermorite and 65 wt% xonotlite) frame. The crystallite size values (30 nm–50 nm) of silicate materials were calculated from X-ray diffraction data using Xfit program and fundamental parameters approach [21].

As material for reinforcement coating the polymer nanocomposite on the base of epoxy resin (Epidian 6),

14 wt% hardener (triethylenetetramine, TETA) and 4 wt% nanosilicate filler (mixture of 35 wt% tobermorite and 65 wt% xonotlite) were used. The mixture of nanofiller and hardener was prepared by dispersing the filler powders in TETA with stirring, followed by sonication for 1 h in Cole-Parmer 8891 ultrasonic bath. Samples were fixed on the set by the prepared polymer nanocomposite. The inside set wall temperature was measured by Type K (chromel/alumel) thermocouples.

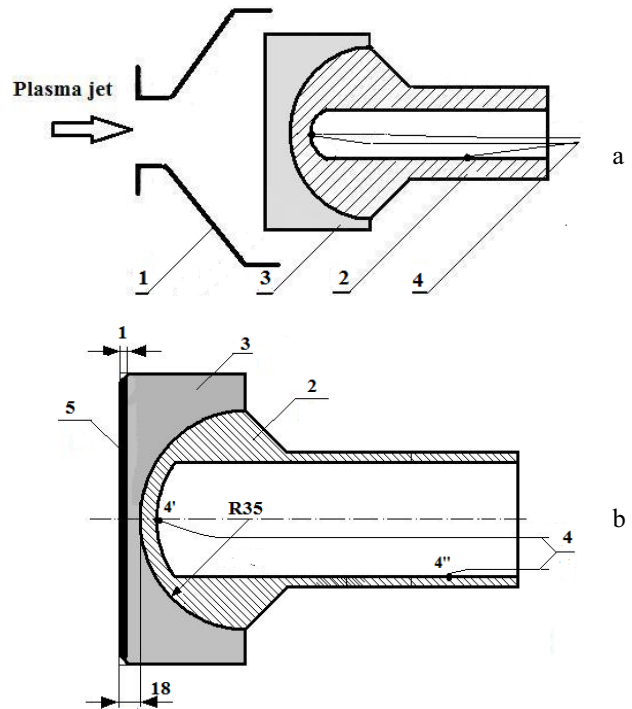


**Fig. 1.** The scheme of the tested sample (a) and geometry of the ablation test body (b): 1 – expanding channel, 2 – set, 3 – protective shell, 4 – thermocouples for measuring shell temperature (4') and set wall temperature (4''), 5 – reinforcement coating

The behavior of the tested shells in plasma jet was observed by a high speed camera. The linear ablation rate  $R$ , defined as the thickness loss per unit time, was defined as [22]:

$$R = \frac{d_1 - d_2}{t}, \quad (1)$$

where  $d_1$  and  $d_2$  represent the thickness of the shell before and after ablation, respectively, and  $t$  being the ablation time. Phase composition of the started material, as well as after the test, was analyzed by XRD. The X-ray diffraction data were collected using the diffractometer DRON-6 (Russian design) in a step scan mode with a step  $\Delta 2\theta = 0.01^\circ$  from  $5^\circ$  to  $70^\circ$   $2\theta$  and the counting time of 1 sec/step. Flat diffracted beam pyrolytic graphite monochromator was used to separate  $\text{CuK}_\alpha$  radiation, and equipment was calibrated by corundum Alfa Aesar  $\alpha\text{-Al}_2\text{O}_3$  (99.9 %) standard.

## 3. RESULTS AND DISCUSSION

Experimental investigations of the ablation resistance of the set with protective shell were provided in two different plasma flows – air plasma jet (sample numbers

N1 and N1C) and combustion gases plasma jet with reduced oxygen content (sample numbers N2 and N2C). Working parameters of the plasma jet reactor for investigation of ablation behaviour of tested samples are presented in Table 1.

**Table 1.** Experimental conditions for plasma ablation test

Sample number	N1	N2	N1C	N2C
Plasma torch capacity, kW	53.1	53.4	53.1	53.4
Gas flow rate, g/s	15.76	17.23	15.76	17.23
Propane flow rate, g/s	0	0.33	0	0.33
Plasma jet temperature, °C	2048	1928	2048	1928

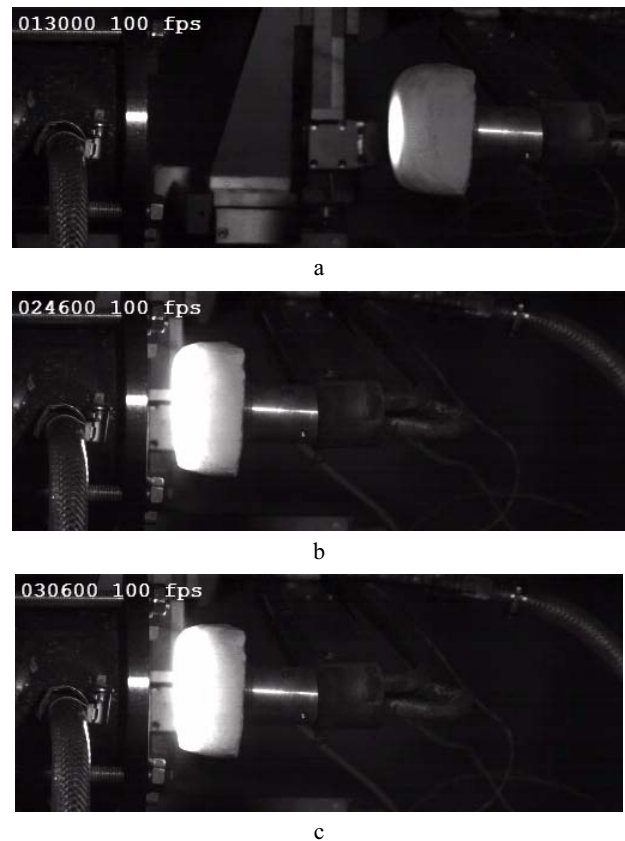
The photographed images made by the highspeed video camera capable of 100 frames per second (fps) was used to evaluate the thickness of the shell removed (Fig. 2). The instantaneous plasma jet images made through the camera window at every 20 s were used for the simulation of the ablation process of the protective shell. The initial image of the shell is presented in Figure 2, a. The next images were photographed every 20 s. The ablation zone became thicker with the prolonged ablation time (Fig. 2, b and c).

Figure 3 shows the ablation rate of coated (N1C and N2C) and uncoated (N1 and N2) protective shell samples as a function of the ablation time in plasma jet. The ablation rate of all samples decreased with the ablation time passed. The linear ablation rate of non-coated sample N2 in the combustion gases plasma flow was 0.036 mm/s during the initial 20 s, and it decreased to 0.015 mm/s when the ablation time exceeded 180 s.

The ablation resistance of the samples with the reinforcement coating is remarkably higher, particularly in the air gas flow environment (N1 and N1C). The existence of the reinforcement coating remarkably decreased the ablation rate of the sample N2C for the first 80 s. The linear ablation rate of the samples tested in plasma flow atmosphere doped with 0.33 g/s propane was higher (N2 and N2C samples). Linear ablation rate (mm/s) of the set after 180 s exposure to plasma jet was 0.005 (N1), 0.015 (N2), 0.005 (N1C) and 0.01 (N2C), respectively.

Thermal performance of the set sample as thermal protection system was investigated by measuring surface

temperatures of the shell and the set. The thermocouples measuring the shell temperature (4') and the set wall temperature (4'') were located in the points presented in Figure 1, b.



**Fig. 2.** Visualization of interaction of protective shell N2C with plasma jet. The recording rate of the camera was 100 fps and the exposure time was 10 μs for each image. The images presented were made after exposure in plasma jet for 0 s (a), 120 s (b) and 180 s (c)

Surface temperatures as a function of exposure time of the set with the protective shell made of silicate composite material are presented in Figure 4. According to the analysis of the temperature dependancies on the samples versus testing time, the shell temperature remains almost time-independent during testing for 180 s in both plasma jet environments (Fig. 4, thick curves 1 and 3).

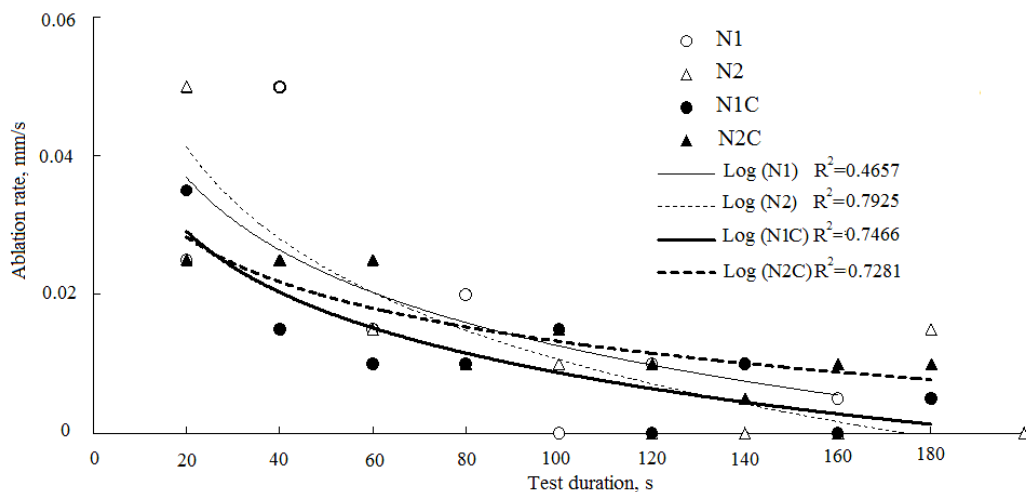


**Fig. 3.** Linear ablation rate of coated and uncoated samples as a function of ablation time

The higher shell temperature of about 150 °C was established for the set tested in plasma jet with the reduced oxygen content (Fig. 4, b) and for the shell with the reinforcement coating tested in air plasma conditions. The best thermal protection was detected for the set with the non-covered silicate-based protective shell (N1). Wall temperature of the set tested in air plasma environment up to 200 s was about 100 °C (Fig. 4, a, 3 curve). Experimental investigations show that the protective shells can protect the surface of the set from high temperature plasma jet up to 250 s under reduced oxygen environment conditions (Fig. 4, b).

Due to the good temperature performance of the shell, the wall temperature of the set is practically independent from the environmental conditions investigated for more than 240 s and its values vary between 130 °C–140 °C (Fig. 4, curves 2 and 4), except the sample N1 (Fig. 4, a, 4 curve) with the less stable set wall temperature versus time and average value of about 80 °C. The wall temperature of the set investigated in air plasma environment is time independent during test time up to 180 s–200 s; meanwhile, the temperature of the set investigated in the reduced oxygen atmosphere is slightly increasing with the prolonged test duration.

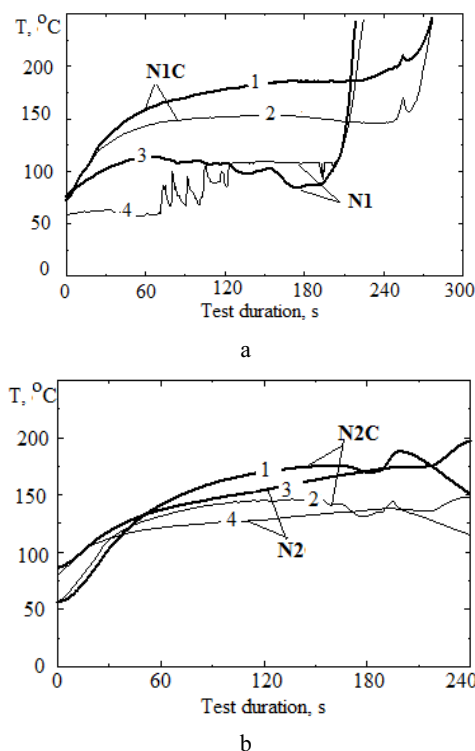


**Fig. 4.** Temperature profiles vs. time during plasma jet testing in air plasma flow (a) and reduced oxygen flow (b): 1, 3 – shell temperature, 2, 4 – set wall temperature. 1, 2 – shell with reinforcement coating, 3, 4 – specimen with non-covered shell

Ablation is a heat and mass transfer process in which a large amount of thermal energy is dissipated to the loss of surface material [23]. According to the results [24], the fused layer at the ablation surface prevents plasma from eroding. The higher values of the shell and set wall temperatures in the case of reinforcement coating can be explained by the exothermic destruction of this coating resulting in additional heating of silicate based shell during

plasma test. It is more evident in the air plasma environment (Fig. 4, a). According to the results obtained, the reinforcement coating serves as the protective layer and helps to enhance the ablation resistance of the shell.

The post-test view of the surface of set N1C after exposure to the ablation testing is presented in Figure 5. The entire thickness of the material was degraded after surface treatment in plasma jet for 240 s.



**Fig. 5.** Surface appearance view of set N1C after exposure to the ablation testing for 240 s

By the XRD analysis two phases of C-S-H – tobermorite and xonotlite were observed in the XRD pattern of the initial test material (Fig. 6, curve 1). After exposure of the material in the plasma jet, the peaks of wollastonite and pseudowollastonite were identified (Fig. 6, curve 2).

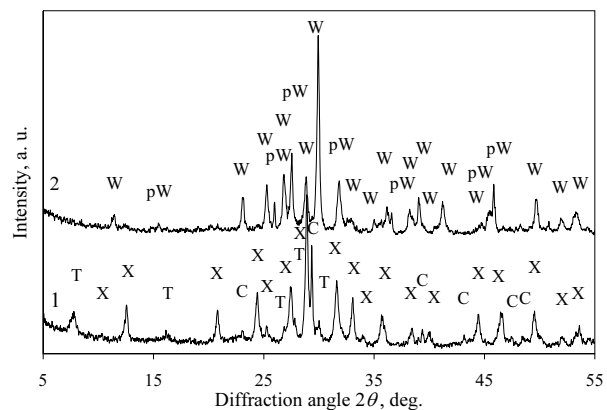


**Fig. 6.** XRD patterns of non-tested set material N1 (curve 1) and after ablation test (curve 2) under plasma jet impact for 200 s. T – tobermorite-11A, X – xonotlite, C – CaCO<sub>3</sub>, W – wollastonite, pW – pseudowollastonite

Tobermorite group minerals are sensitive to CO<sub>2</sub> gas which considerably changes their mineralogical composition and properties [25]. By their results, during the initial stage of tobermorite carbonization, a CaCO<sub>3</sub> modification – vaterite, is formed. Over the extended period it is regrouped into a calcite (Fig. 6, curve 1). It is thought [25] that destruction of tobermorite structure requires humidity. Xonotlite is more resistant silicate material to carbonisation [26].

The research [26] showed the dehydration of xonotlite to low-T-wollastonite at about 800 °C. Low-T-wollastonite transforms to high-T-wollastonite (pseudowollastonite) at about 1125 °C by a reconstructive phase transition. When tobermorite is heated to ~900 °C, wollastonite is produced, but when carbonated tobermorite was heated, the products were pseudo-wollastonite and wollastonite (Fig. 6, curve 2). These results coincide with the investigations

presented in [26, 27]. Due to the high melting point, wollastonite is suitable as high temperature stable reinforcement coating. Low coefficient of thermal expansion of wollastonite warrants high thermal shock resistance and dimensional stability of wollastonite based material for high temperature applications.

#### 4. CONCLUSIONS

The light silicate shell has demonstrated good resistance to the impact of high temperature gas flow initiated by plasma jet. The additional impregnation of light silicate shell with epoxy nanocomposite reinforcement coating increased the temperature on the shell surface due to exothermic reactions but decreased the ablation rate accordingly. The experiments in reduced oxygen flow have shown good thermal stability of the protective shell.

Finally, the wollastonite as high temperature resistance substance was obtained in the protective shell structure. Wollastonite structure imparts high thermal shock resistance and dimensional stability for the protective shell in high temperature applications.

#### Acknowledgments

The authors acknowledge the Research Council of Lithuania and partners of COST MP0701 Action for the support of this research.

#### REFERENCES

1. Valente, T., Bartuli, C., Pulci, G. Ceramic Composites and Thermal Protection Systems for Reusable Re-entry Vehicles *Advances in Science and Technology* 45 2006: pp. 1505–1514.
2. Venkatapathy, E. et al. Thermal Protection System Development, Testing, and Qualification for Atmospheric Probes and Sample Return Missions. Examples for Saturn, Titan and Stardust-type Sample Return *Advances in Space Research* 44 2009: pp. 138–150.
3. Savino, R. et al. Arc-jet Testing on HfB<sub>2</sub> and HfC-based Ultra-high Temperature Ceramic Materials *Journal of the European Ceramic Society* 28 2008: pp. 1899–1907. <http://dx.doi.org/10.1016/j.jeurceramsoc.2007.11.021>
4. Ceramics in Aerospace, <http://www.ceramics-directory.com>.
5. Aluminium Silicate, <http://www.morgantechceramics.com>.
6. Mojumdar, S. C. et al. Thermal, Spectral and AFM Studies of Calcium Silicate Hydrate-Polymer Nanocomposite Material *Journal of Thermal Analysis and Calorimetry* 85 (1) 2006: pp. 119–124. <http://dx.doi.org/10.1007/s10973-005-7354-8>
7. Shuyuan, Z., Boming, Z., Shanyi, D. Effects of Contact Resistance on Heat Transfer Behaviors of Fibrous Insulation *Chinese Journal of Aeronautics* 22 (5) 2009: pp. 569–574.
8. Shukla, K. N., Pradeep, A., Suneesh, S. S. Thermal Performance Analysis of Silica Tiles *Journal of Engineering Physics and Thermophysics* 79 (6) 2006: pp. 1157–1163.
9. Zhao, S., Zhang, B., He, X. Temperature and Pressure Dependent Effective Thermal Conductivity of Fibrous Insulation *International Journal of Thermal Sciences* 48 2009: pp. 440–448.
10. Ritter, H. Development of a European Ablative Material for Heatshields of Sample Return Missions *Proc. of 6th European Workshop on Thermal Protection Systems and Hot Structures* Stuttgart, Germany, 1–3 April 2009: p. 19.
11. Shih, Y.C. et al. Numerical Study of Transient Thermal Ablation of High-Temperature Insulation Materials *Journal of Thermophysics and Heat Transfer* 17 (1) 2003: pp. 53–60. <http://dx.doi.org/10.2514/2.6733>
12. Grabow, R. Ablative Heat Shielding for Spacecraft Re-entry, San Diego, 2006: 15 p.
13. Monti, R., De Stefano Fumo, M., Savino, R. Thermal Shielding of a Reentry Vehicle by Ultra-High Temperature Ceramic Materials *Journal of Thermophysics and Heat Transfer* 2036 (3) 2006: pp. 500–506. <http://dx.doi.org/10.2514/1.17947>
14. Leszczyńska, A., Njuguna, J., Pielichowski, K., Banerjee, J. R. Polymer/montmorillonite Nanocomposites with Improved Thermal Properties *Thermochimica Acta* 453 (2) 2007: pp. 75–96.
15. Stewart, J. D., Greenshields, D. H. Entry Vehicles for Space Programs *Journal of Spacecraft and Rockets* 6 (10) 1969: pp. 1089–1113.
16. Stahl, B., Emunds, H., Gulhan, A. Experimental Investigation of Hot and Cold Side Jet Interaction with a Supersonic Cross-flow *Aerospace Science and Technology* 13 2009: pp. 488–496.
17. Dkz, J., Hernindez, S. Uncertainty Quantification and Robust Design of Aircraft Components under Thermal Loads *Aerospace Science and Technology* 14 2010: pp. 227–534.
18. Li, G. et al. Ablation Resistance of ZrB<sub>2</sub>-SiC-AlN Ceramic Composites *Journal of Alloys and Compounds* 479 2009: pp. 299–302. <http://dx.doi.org/10.1016/j.jallcom.2008.12.036>
19. Valinčius, V., Krušinskaitė, V., Valatkevičius, P., Valinčiūtė, V. Electric and Thermal Characteristics of the Linear, Sectional DC Plasma Generator *Plasma Sources Science and Technology* 13 2004: pp. 199–206. <http://dx.doi.org/10.1088/0963-0252/13/2/002>
20. Valinčiūtė, V., Kėželis, R., Valinčius, V., Valatkevičius, P., Mėčius, V. Heat Transfer in Plasma Jet Reactor for Melting and Melt Fibrillation of Hard Ceramics *Advances in Heat Transfer: Proc. of the Baltic Heat Transfer Conf.* 2 2007: pp. 580–588.
21. Cheary, R. W., Coehlo, A. A. Programme XFIT and Fourya. Deposited in CCP14 Powder Diffraction Library. Engineering and Physical Science Research Council. Daresbury Laboratory, Warrington, England, 1996.
22. Song, G. M. et al. Ultra-high Temperature Ablation Behavior of Ti<sub>2</sub>AlC Ceramics under an Oxyacetylene Flame *Journal of the European Ceramic Society* 31 2011: pp. 855–862.
23. Jiang, Y. G. et al. Ablation and Radar-wave Transmission Performances of the Nitride Ceramic Matrix Composites *Science in China Series E: Technological Sciences* 51 (1) 2008: pp. 40–45. <http://dx.doi.org/10.1007/s11431-007-0062-9>
24. Bahramian, A. R., Kobaki, M. Ablation Mechanism of Polymer Layered Silicate Nanocomposite Heat Shield *Journal of Hazardous Materials* 166 2009: pp. 445–454.
25. Siauciunas, R., Rupsyte, E., Kitrys, S., Galeckas, V. Influence of Tobermorite Texture and Specific Surface Area on CO<sub>2</sub> Chemisorption *Colloids and Surfaces A: Physicochemical and Engineering Aspects* 244 2004: pp. 197–204. <http://dx.doi.org/10.1016/j.colsurfa.2004.06.004>
26. Vektaris, B., Vilkas, V. Stability of Concrete. Kaunas, Technologija, 2006: 162 p.
27. Spudulis, E., Šavareika, V. The Influence of the Suspension Concentration and Different Mixing Intensity to the Synthesis of Xonotlite *Cheminė technologija ISSN 1392-1231* 2 (51) 2009: pp. 44–50 (in Lithuanian).

Presented at the 20th International Baltic Conference "Materials Engineering 2011" (Kaunas, Lithuania, October 27–28, 2011)